Phase diagrams and morphology of polymer dispersed liquid crystals based on nematic-liquid-crystal–monofunctional-acrylate mixtures

Frédérick Roussel* and Jean-Marc Buisine
Laboratoire de Thermophysique de la Matière Condensée, Equipe de l'UPRESA CNRS 8024, Université du Littoral-Côte d'Opale, MREID, 59140 Dunkerque, France

Ulrich Maschke and Xavier Coqueret
Laboratoire de Chimie Macromoléculaire, UPRESA CNRS 8009, Université des Sciences et Techonologies de Lille, 59655 Villeneuve d'Ascq, France

Farida Benmouna
Institut de Physique et de Chimie, Université Aboubakr Belkaïd, Bel Horizon BP119, 13000 Tlemcen, Algeria
(Received 22 November 1999; revised manuscript received 14 March 2000)

Phase diagrams of unpolymerized and UV-polymerized 2-ethyl hexyl acrylate (EHA) mixtures with the liquid crystal E7 are established using optical microscopy and differential scanning calorimetry. Both diagrams show upper critical solution temperature behavior. From 50 to 90 wt % liquid crystal (LC), the (I+I) phase located between the (N+I) and (I) phases was clearly shown. The nematic phase inside the droplets exhibits a twisted radial structure indicating that homeotropic anchoring occurs at the polymer interface. The experimental phase diagrams were successfully analyzed using a model based on the Flory-Huggins theory of isotropic mixing supplemented with the Maier-Saupe theory of nematic order. The LC solubility limit in the polymer matrix and the fractional amount of LC contained in the droplets were deduced from the calorimetric measurements. For the specific composition EHA/E7 (50:50), the scattering and morphological properties of the films were studied as a function of time elapsed after UV exposure. Drastic changes in the size, shape, spatial distribution, and number density of nematic droplets were observed and analyzed in terms of coalescence/diffusion phenomena.

PACS number(s): 61.30.−v, 64.70.Md, 64.75.+g, 42.70.Df

I. INTRODUCTION

In the last few years, polymer dispersed liquid crystals (PDLC's) have received particular attention due to their considerable potential for electro-optical applications such as flexible displays and switchable windows [1,2]. In their most common form, PDLC films consist of low molecular weight liquid crystals (LC's) dispersed as micrometer-sized droplets within a solid polymer matrix. One way to prepare PDLC's is polymerization-induced phase separation (PIPS), which occurs when a homogeneous mixture of monomers and LC's is polymerized. UV-induced polymerization is a preferred method because the curing parameters can be chosen independently [3,4]. The phase separation process and the phase behavior are the main aspects governing the morphology of PDLC films. Indeed, the size, shape, spatial distribution, and number density of LC droplets in particular influence the electro-optical properties of these films.

Theoretical equilibrium phase diagrams for various hypothetical LC/polymer systems have been studied to understand the phase properties of such mixtures [5–9]. Particular interest has been given to the experimental determination of phase diagrams. Kyu and co-workers investigated the phase behavior of polybenzylmethacrylate (PBMA)/E7 [5], polystyrene (PS)/E7 [6], polymethylmethacrylate (PMMA)/E7 [7], and functionalized PMMA/E7 [8], whereas Carpaneto *et al.* [10] studied the poly-*n*-butylmethacrylate/E7 and PMMA/E7 systems. The cloud point curves observed by polarized optical microscopy (POM) and/or light scattering (LS) were usually reported by these authors. Using POM, LS, and differential scanning calorimetry (DSC) techniques, Ahn *et al.* [11] performed a more detailed investigation of the phase diagrams of PMMA and PS in mixtures with the liquid crystal 7CB. Nematic (N), nematic-isotropic (N+I), isotropic-isotropic (I+I) and isotropic (I) phases have been observed by these authors. Recently, Benmouna *et al.* [12] studied the phase behavior of various blends including different monodisperse PS's and a LC exhibiting a smectic-*A* phase (8CB). The (I), (I+I), (N+I), and smectic-*A*–isotropic (S_A+I) phases were identified. A good agreement between the experimental data and the theoretical predictions of the phase diagrams was obtained. The influence of the PS molecular weight on the LC solubility was also shown.

The previously mentioned studies were conducted by a solvent-induced phase separation mechanism followed by a thermally induced phase separation process. The phase diagrams of linear homopolymer/LC blends have already been reported in the literature but to our knowledge not in the case of blends prepared by the PIPS process. Only phase diagrams of mixtures in the unpolymerized state, i.e., before undergoing a PIPS process, have been [13–16].

In this paper, experimental phase diagrams for mixtures of 2-ethyl hexyl acrylate (EHA) with E7 covering a wide

*Author to whom correspondence should be addressed. Email address: roussel@univ-littoral.fr

concentration range of LC are presented. Section II describes the preparation of the samples and explains how the experiments are carried out. In Sec. III A the phase behavior of unpolymerized blends is investigated by POM and analyzed in terms of a classical model based on a combination of the Flory-Huggins (FH) theory of isotropic mixing [17] and the Maier-Saupe (MS) theory of nematic order [18]. From POM and DSC analysis the phase properties of PDLC samples prepared using a photoinitiated PIPS process are described in Sec. III B and the phase diagram obtained is interpreted using the FH and MS model. The LC solubility limit and the fractional amount of LC contained in the droplets are also estimated. Section III C deals with the transmission and morphological properties of the polymerized films EHA/E7 (50:50) as a function of time elapsed after UV exposure. A brief conclusion closes the paper.

II. EXPERIMENT

The liquid crystalline mixture E7 (Merck, Nogent, France) was used during this work. E7 exhibits a nematic phase at room temperature, which easily forms a glassy nematic upon cooling, and crystallization does not readily occur upon reheating. The glass gradually becomes a fluid nematic at $T_{g_{E7}} = -62\,^{\circ}\mathrm{C}$ [19]. The nematic-isotropic transition of E7 occurs at $T_{NI} = 61\,^{\circ}\mathrm{C}$ [20] with $\Delta H_{NI} = 4.5\ \mathrm{J\ g^{-1}}$ [19]. The monofunctional acrylate monomer 2-ethyl hexyl acrylate was used as precursor of the homopolymer. EHA was supplied from Aldrich (Saint Quentin Fallavier, France) and used without further purification. The UV polymerization was induced by 2 wt % of Darocur 1173 (Ciba, Rueil Malmaison, France) with respect to the amount of monomer used.

The monomer and the liquid crystal were mixed together at room temperature for several hours. Samples for optical microscopy were prepared by placing one drop of the mixture between standard glass slides resulting in a film thickness of approximately $3\,\mu$m. Samples for calorimetric measurements were prepared by introducing 2.9 ± 0.1 mg of PDLC precursors into aluminum DSC pans, which were sealed after UV exposure to avoid evaporation effects during the temperature treatment.

The photopolymerization process was carried out in the DSC furnace under isothermal conditions ($T = 25\,^{\circ}\mathrm{C}$) and nitrogen atmosphere. The wavelength of the UV lamp (Hg-Xe) was fixed at $\lambda = 365$ nm using interferential filters. The UV irradiation intensity was 17.5 mW cm^{-2} and the irradiation time was set at 3 min [21].

Using the previously described UV-irradiation method, four pure EHA samples (without E7) were polymerized between standard glass slides. The molecular weights and the polydispersities of the PEHA films obtained were determined by gel permeation chromatography (GPC) calibrated with PS standards. GPC measurements were performed in tetrahydrofuran (THF) at room temperature yielding $M_w = 108\,000 \pm 5000$ g mol^{-1} and $M_w/M_n = 2.1 \pm 0.2$. These results present averages from one GPC measurement performed on each of the four PEHA samples.

The polarized optical microscopy studies were performed on a Leica DMRXP microscope equipped with a heating/cooling stage (Chaixmeca). The phase diagram of the unpolymerized mixtures EHA/E7 was obtained by using the following temperature treatment. Samples were first heated from room temperature to a temperature located 15 °C above the isotropic phase limit, then quenched at 100 °C min^{-1} to $-100\,^{\circ}\mathrm{C}$. Subsequently, another heating cycle with a rate of 5 °C min^{-1} up to the isotropic state was carried out. After UV irradiation, PDLC samples, denoted PEHA/E7, were studied in a similar way. From room temperature, the samples were heated at 5 °C min^{-1} to a temperature located 15 °C above the isotropic state, then cooled down at a rate of $-1\,^{\circ}\mathrm{C\,min^{-1}}$ to a temperature situated 15 °C below the (N+I)-(I) or (I+I)-(I) transition line. Then a heating cycle at a rate of 1 °C min^{-1} up to the isotropic state was carried out. For both unpolymerized and polymerized mixtures two independent samples of the same composition were analyzed. The reason for choosing several heating/cooling cycles is to make preliminary observations of the transition temperatures. Final recording of these temperatures was made at the third heating ramp. The rate of heating during the final ramp was different for the unpolymerized (5 °C min^{-1}) and UV-polymerized samples (1 °C min^{-1}). These rates were chosen in a search for the most favorable conditions that allow clear identification of the transition temperature corresponding to morphology changes of the phases. These conditions were imposed by the requirement to reach the equilibrium state of the system. Figure 2 below displays the textures in the (N+I) and (I+I) regions and gives an example of texture changes in the transition from (N+I) to (I+I). For lower heating ramps in both systems, the transition temperatures were not modified, meaning that the system had reached equilibrium.

The DSC measurements carried out on the polymerized blends PEHA/E7 were performed on a Seiko DSC 220C equipped with a liquid nitrogen system allowing cooling experiments. The DSC cell was purged with 50 ml min^{-1} of nitrogen. Rates of 10 °C min^{-1} (heating) and 30 °C min^{-1} (cooling) were used in the temperature range -120 to 100 °C. The method consists in first cooling the samples prior to heating and cooling cycles. This procedure enables one to detect the transition temperature unambiguously and leads to a reduction in the peak width of those transitions shown in the thermograms. Data analysis was carried out during the second heating ramp. The glass transition temperature (T_g) of the PEHA/E7 system was measured from the midpoint of the transition range of the thermogram, whereas the peaks of the clearing points were used to determine the nematic-isotropic transition temperature T_{NI} [22].

After UV irradiation, the light transmission ratio I_T/I_0 of PDLC films including 50 wt % E7 was investigated by measuring the transmitted light of a HeNe laser operating at a wavelength of $\lambda = 632.8$ nm. The PDLC samples (thickness 3 μm) sandwiched between two glass plates were placed normal to the laser beam. The distance between the sample cell and the silicon photodiode was approximately 15 cm. The collection angle of the forward transmitted light was set to about 2° by an iris.

III. RESULTS AND DISCUSSION

A. Phase diagram before polymerization

It has been established [3,15,16] that knowledge of the phase behavior of prepolymer/LC systems is essential for

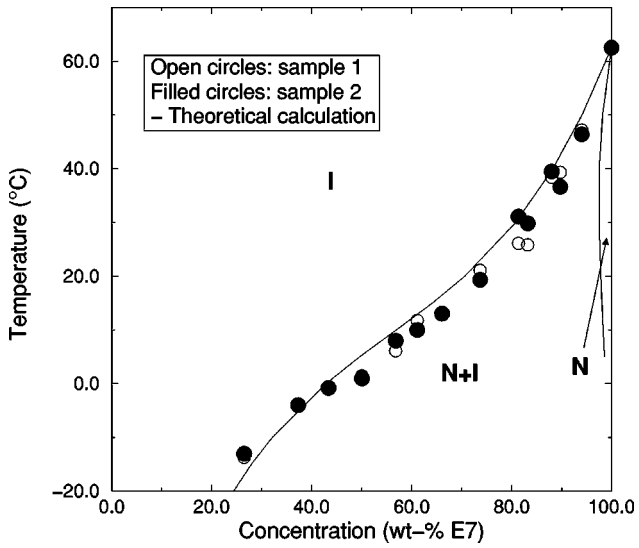

FIG. 1. Phase diagram of the unpolymerized mixtures EHA/E7 obtained from polarized optical microscopy; two domains are experimentally observed: isotropic (I), and nematic + isotropic (N + I). The solid lines correspond to the theoretical predictions using $N_1=1$, $N_2=2$, and $\chi=-1.35+685/T$.

PDLC preparation because it gives the thermodynamic stability of the starting mixture as a function of temperature and composition. Amundson *et al.* [16] demonstrated that these two parameters combined with the degree of polymerization during cure have strong effects on the droplet growth, film morphology, and electro-optical properties. Therefore the phase properties of unpolymerized EHA/E7 blends were investigated by POM on heating. The experimental phase diagram is shown in Fig. 1. The open symbols represent the first sample whereas the filled symbols correspond to the results obtained from the second sample. These data show the transition from (N+I) to (I) regions. The continuous line is the calculated coexistence curve using the model described hereafter. The two coexisting phases (N+I) for the unpolymerized system were observed by the POM technique. The nematic phase consists of spherical droplets dispersed in the isotropic monomer rich phase (black background in the micrographs). Since the micrograph obtained in this region closely resembles the one in the analogous region of the polymerized samples shown in Fig. 2 (bottom), it would be redundant to give both of them here. The single nematic phase shown on the right hand side of Fig. 1 is a theoretical prediction but such a nematic phase has not been observed with the experimental techniques used here.

These results are in good agreement with those reported in the literature. Hirai *et al.* [14] found a similar phase diagram for ethyl hexyl acrylate/urethane diacrylate/E8 mixtures as well as Smith [13] for NOA65/E7 blends. As for the previously mentioned studies, the monomer/isotropic LC two-phase state (I+I) was not observed.

The phase diagram of the unpolymerized EHA/E7 mixture is constructed starting from the free energy density

$$f=f_{FH}+f_{MS}, \tag{3.1}$$

where f_{FH} is the Flory-Huggins free energy [17],

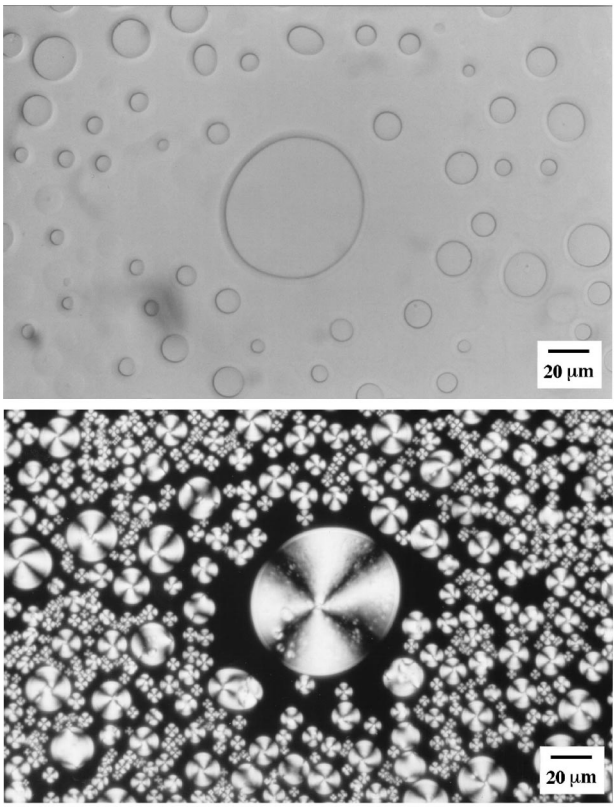

FIG. 2. Optical micrographs of PEHA/E7 (35:65). Top: $T=62.3\,^{\circ}\mathrm{C}$, $P\|A$, (I+I) region; bottom: $T=45.0\,^{\circ}\mathrm{C}$, $P\perp A$, (N +I) region. An isotropic polymer rich phase is in equilibrium with an isotropic LC phase at $T>T_{NI}$ (top) and with a nematic LC phase at $T<T_{NI}$ (bottom).

$$\frac{f_{FH}}{k_BT}=\frac{\varphi_1}{N_1}\ln\varphi_1+\frac{\varphi_2}{N_2}ln\ \varphi_2+\chi\varphi_1\varphi_2. \tag{3.2}$$

k_BT is the thermal energy, φ_1 is the volume fraction of the LC E7, and φ_2 the volume fraction of EHA; N_1 and N_2 are the numbers of repeat units of the LC and the polymer, respectively; χ is the Flory-Huggins interaction parameter for isotropic mixing. The Maier-Saupe free energy [18] is

$$\frac{f_{MS}}{k_BT}=\frac{\varphi_1}{N_1}\left(-\ln Z+\frac{1}{2}\nu\varphi_1S^2\right), \tag{3.3}$$

where ν is the Maier-Saupe quadrupole interaction parameter

$$\nu=4.54\frac{T_{NI}}{T}. \tag{3.4}$$

The nematic order parameter S is a function of temperature and composition. The nematic-isotropic transition temperature T_{NI} is known for the pure LC E7 to be $T_{NI}=61\,^{\circ}\mathrm{C}$. In Eq. (3.3), Z is the nematic partition function. The binodal curve is calculated following the standard procedure of chemical potential equality in coexisting phases. This calculation gives the solid line of Fig. 1, which is calculated using the parameters $N_1=1$, $N_2=2$, and $\chi=-1.35+685/T$. A good agreement is obtained between experimental data and theoretical predictions concerning the transition temperature from the (N+I) to the (I) region.

Even if the liquid crystal employed is a eutectic mixture, the use of the binary phase diagram offers several important pieces of information, including the monomer/LC demixing curve. The EHA/E7 system is miscible over a wide temperature and concentration range. For LC content from 35 to 70 wt %, the coexistence curve (N+I)-(I) is close to the curing temperature (25 °C), meaning that the phase separation will occur early in the polymerization process [3,15,16]. In other words, the LC droplets will form as soon as the molecular weight of the acrylate component increases.

B. Phase properties of PDLC samples

Figure 2 represents optical micrographs of PEHA/E7 (35:65) at $T=45.0$°C using the crossed polarizer mode (bottom) and $T=62.3$°C where polarizer (P) and analyzer (A) were oriented parallel to each other (top). The (N+I) phase is present in Fig. 2 (bottom) whereas Fig. 2 (top) shows unambiguously the (I+I) morphology.

Through crossed polarizers, the nematic drops [Fig. 2 (bottom)] exhibit a twisted radial structure [23], indicating that the LC molecules adopt a homeotropic anchoring at the polymer interface. This observation is in good agreement with previous work on alkyl brush surfaces and liquid crystal anchoring transitions at surfaces [24–26]. It has been demonstrated that a high density of alkyl chains, like the 2-ethyl hexyl groups on the PEHA polymer backbone, attached to an interface induces homeotropic anchoring. Indeed, interdigitation between alkyl ends of mesogens and alkyl brush is best achieved when the mesogens are perpendicular to the surface [24]. For LC content above 95 wt %, no (I+I) region was observed. This behavior has already been discussed in the literature [11,27] and attributed to the difficulty of distinguishing experimentally the transitions (N+I)-(I) and the (N+I)-(I+I). Dubault *et al.* [27] have shown that the phase separation process for polymer/LC mixtures with low polymer concentrations may require several days, which is beyond the time scale used for our experiments.

The DSC thermal spectra for the polymerized PEHA/E7 mixtures with various LC contents are shown in Fig. 3. At low temperature ($T\sim -60$ °C), the glass transition temperatures of the polymer $T_{g_{PEHA}}$ and the LC $T_{g_{E7}}$ overlap, leading to a unique transition in the whole concentration range. Beyond the glass transition temperature, the DSC thermograms of the samples containing a finite amount of polymer exhibit bumps due probably to some unknown weak transitions of the polymer. These bumps do not extend over the region near the nematic to isotropic transition temperature T_{NI} of the liquid crystal and therefore they have no significant effect on the phase behavior of the mixtures under investigation in the range of temperatures of practical interest. For all samples of composition above 50 wt % E7, the nematic to isotropic transition is clearly observed and remains nearly constant $T_{NI}\sim 61$ °C, representing roughly the same value as that of the pure LC. These observations indicate that the phase separated LC is essentially pure and not contaminated by remaining monomer. For lower LC content ranging from 30 to 50 wt %, the nematic to isotropic transformation becomes diffuse and exhibits a positive baseline shift (exotherms are upward going). These shifts can be explained by an excess specific heat of mixing $\Delta C_{p_{mix}}$ of the polymer and the LC

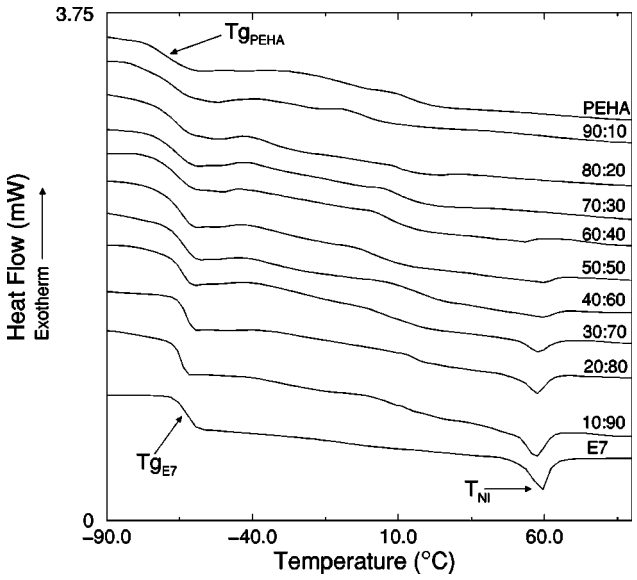

FIG. 3. Thermograms obtained from DSC measurements (heating rate 10 °C/min) for a series of polymerized PEHA/E7 mixtures for LC concentrations ranging from 0 to 100 wt %. $T_{g_{PEHA}}$ and $T_{g_{E7}}$ are the glass transition temperatures of the polymer and the liquid crystal, respectively, and T_{NI} is the nematic to isotropic transition temperature.

overlapping with the nematic to isotropic transition. Previous studies on blends of polymers and mixtures of monomers and LC's have shown that $\Delta C_{p_{mix}}$ is positive for upper critical solution temperature (UCST) phase diagrams [13,28,29]. Our results obtained for linear polymer/nematic LC are therefore consistent with the previously published work. The (I+I)-(I) transition cannot be observed by DSC analysis since this transition is accompanied by a very small enthalpy change.

Figure 4 shows the phase diagram for the polymerized mixture PEHA/E7 in the form of temperature versus LC weight fraction. The symbols represent POM and DSC data as indicated in the figure legend, while the solid line is the theoretical coexistence curve obtained from the model described earlier. DSC data obtained for the nematic to isotropic transition temperature T_{NI} are in reasonable agreement with the POM measurements. However, it can be observed that DSC thermograms give slightly lower transition temperatures than those obtained from POM. In the pure LC state, POM measurements give $T_{NI}=62.5$ °C whereas DSC data yield $T_{NI}=59.6$ °C. Approximately the same difference can also be measured for PEHA/E7 blends in the range from 60 to 100 wt % of LC. This discrepancy is probably due to differences in the methods of analysis and sample preparation. The diagram exhibits an upper critical solution temperature shape with three distinct regions. Above the solid line, the system present a single isotropic (I) phase while below one observes two biphasic (N+I) and (I+I) regions. The diagram exhibits a triple point at $T=61$ °C, where two isotropic phases with different polymer concentrations coexist with a pure nematic liquid crystal phase. Below the dashed line an isotropic polymer rich phase is in equilibrium with a nematic LC phase (say, β). Since the composition of the β phase is known ($\varphi_1^{\beta}=1$), it is sufficient to solve the single equation $\mu_1^{\alpha}=\mu_1^{\beta}$ where the liquid crystal dispersed in the α

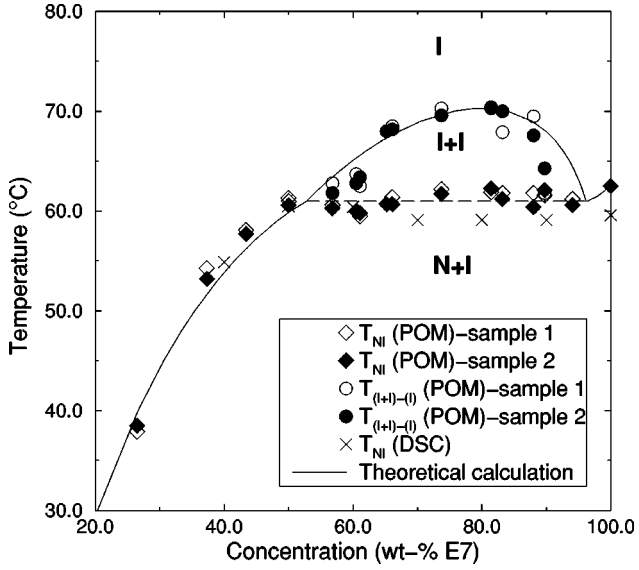

FIG. 4. Phase diagram of PEHA/E7 obtained from POM and DSC techniques. T_{NI} represents the transition temperature of the phase separated liquid crystal between the nematic and isotropic states and $T_{(I+I)\text{-}(I)}$ is the (isotropic + isotropic) to isotropic transition temperature. Three domains are observed: nematic + isotropic (N+I), isotropic + isotropic (I+I), and isotropic (I). The solid line is calculated from the Flory-Huggins and Maier-Saupe free energies using $N_1=1$, $N_2=16$, and $\chi=-2.49+1123/T$.

phase is isotropic while that of the β phase is nematic. The solution of this equation yields the composition of the α phase. Above the dashed line, the phase diagram shows an isotropic miscibility gap (I+I). Here, one needs to solve the set of equations

$$\mu_1^{\alpha}=\mu_1^{\beta}, \quad \mu_2^{\alpha}=\mu_2^{\beta} \tag{3.5}$$

to obtain the composition of the two phases in equilibrium. The parameters used to construct the theoretical phase diagram are $N_1=1$, $N_2=16$, and $\chi=-2.49+1123/T$. Only one fit parameter was used. N_1 was set to 1, assuming that low molecular weight LC is made of only one repeat unit, which is a reasonable assumption. N_2 was obtained from the experimental critical composition $\varphi_c=0.795$ using the mean field result

$$\varphi_c=\frac{\sqrt{N_2}}{\sqrt{N_1}+\sqrt{N_2}}. \tag{3.6}$$

The true value of N_2 is certainly higher than 16. This discrepancy is probably due to an incertitude in determining the critical volume fraction at the maximum of the experimental coexistence curve. Slightly higher φ_c values will immediately yield much higher N_2 values in this range of LC composition. It should also be noted that the photopolymerization process of EHA/E7 mixtures can be altered by the diluting effect of the LC molecules, leading to polymer chains with fewer repeat units [4]. The value of φ_c can be used to determine the critical parameter χ_c,

$$\chi_c=\frac{1}{2}\left(\frac{1}{\sqrt{N_1}}+\frac{1}{\sqrt{N_2}}\right)^2. \tag{3.7}$$

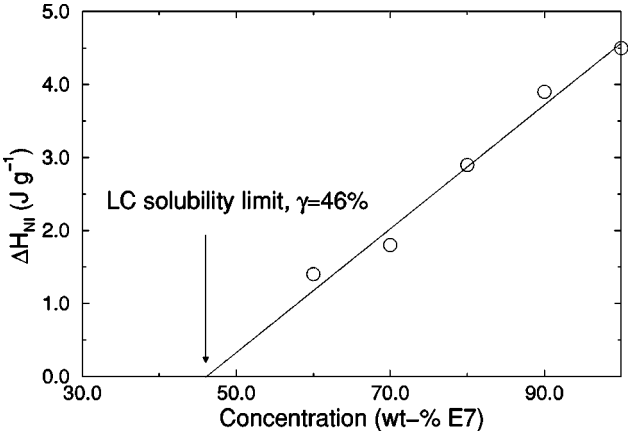

FIG. 5. Enthalpy changes at the nematic-isotropic transition versus E7 concentration. The LC solubility limit in the polymer matrix, γ, was determined by linear regression of the experimental data set followed by calculating the x-axis intercept.

Knowing the critical temperature $T_c=70.5\,^{\circ}\mathrm{C}$ and recalling that

$$\chi_c=A+\frac{B}{T_c} \tag{3.8}$$

gives

$$B=(\chi_c-A)T_c. \tag{3.9}$$

Only the parameter A remains to be fixed in order to fit the data. This procedure leads to the solid line in Fig. 4 and shows that there is a quite good agreement between the experimental data and the calculated curve.

The solubility limit γ of the LC molecules in the polymer and the relative amount δ of LC in the nematic droplets are other interesting properties that can be deduced from the phase diagram and the thermodynamic quantities accessible from the DSC data. According to Smith and Vaz [30] and Maschke *et al.* [31], γ can be related to the nematic-isotropic enthalpy ΔH_{NI}:

$$P(x)=\frac{x-\gamma}{100-\gamma}, \quad \text{with} \quad P(x)=\frac{\Delta H_{NI}(x)}{\Delta H_{NI}(\mathrm{LC})}. \tag{3.10}$$

$P(x)$ represents the ratio of the nematic-isotropic transition enthalpy for a LC/polymer composite material to the equivalent value for the pure LC. This expression is based on the following assumptions: (i) the LC in the droplets exhibits the same thermophysical behavior as in the bulk state; (ii) the amount of LC dissolved in the polymer is constant for LC concentrations $x \geqslant \gamma$ and does not contribute to ΔH_{NI}; (iii) the T_{NI} values as a function of x remain unchanged, so that ΔH_{NI} is not influenced by the presence of polymer molecules dissolved in the LC droplets; (iv) the densities of the polymer precursors and the LC are approximately equal.

The effects of the LC concentration on ΔH_{NI} are presented in Fig. 5. $\Delta H_{NI}(x)$ increases linearly with x, validating the model given in Eq. (3.10). The LC solubility limit γ was determined by linear regression of the experimental data set in Fig. 5 followed by calculating the x-axis intercept. The

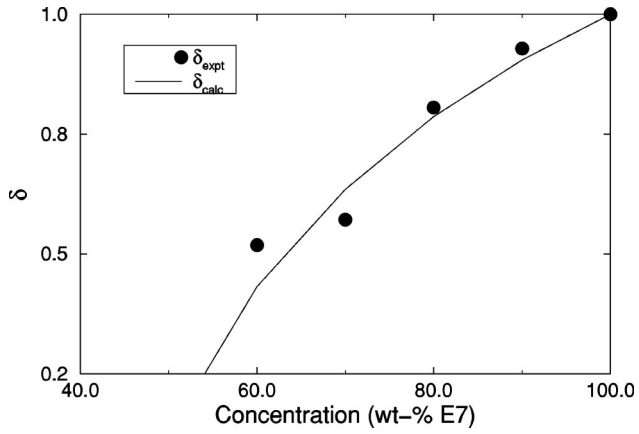

FIG. 6. Dependence of the fractional amount of LC contained in microdroplets, δ, on the E7 concentration. The filled circles represent the experimental values deduced from Eq. (3.11) and the solid line is a calculated curve using Eq. (3.12).

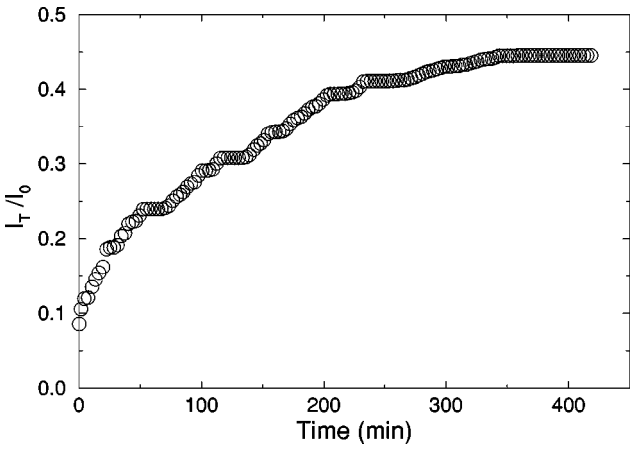

FIG. 7. Light transmission ratio I_T/I_0 of PEHA/E7 films as a function of time elapsed after UV exposure ($\lambda = 632.8$ nm, $T = 25\,^{\circ}\mathrm{C}$).

value of γ was 46%, which is comparable to that of linear homopolymer/LC mixtures, such as PS/E7, PMMA/E7 [11], and PS/8CB [12].

ΔH_{NI} can be used to calculate δ_{expt}, the LC fraction contained in the droplets [19,30,31]:

$$\delta_{expt} = \frac{m_{LC}^{D}}{m_{LC}} = \left(1 + \frac{m_P}{m_{LC}}\right) P(x) = \left(\frac{100}{x}\right) P(x), \quad (3.11)$$

where m_{LC}^{D} represents the mass of LC included in the droplets, while m_P and m_{LC} are the masses of the polymer and the LC in the sample, respectively. Combining Eqs. (3.10) and (3.11) yields

$$\delta_{calc} = \left(\frac{100}{x}\right)\left(\frac{x-\gamma}{100-\gamma}\right), \quad x \geqslant \gamma. \quad (3.12)$$

Figure 6 illustrates the dependence of δ on the LC concentration. The filled circles represent δ_{expt} values determined for each composition by applying Eq. (3.11), whereas the solid line was calculated (δ_{calc}) by using the previously mentioned γ values and Eq. (3.12). At the miscibility limit, x is equal to γ and δ is zero, consistent with Eq. (3.12). When x increases, δ_{expt} also increases rapidly. Experimental values and calculated curves are in good agreement.

C. Transmission and morphology of PEHA/E7 (50:50) films as a function of time elapsed after UV exposure

The scattering properties and the morphology of PEHA/E7 (50:50) films as a function of time elapsed after UV exposure have been investigated by light transmission measurements and POM observations. For a collection of droplets that scatter independently, the intensity of a collimated light source through a PDLC sample can be expressed by writing [1,32]

$$I_T = I_0 \exp(-\sigma d), \quad (3.13)$$

where I_T is the transmitted intensity, I_0 the incident intensity, d the sample thickness, and σ the scattering cross section. Figure 7 shows the variation of the ratio I_T/I_0 as a function of time elapsed after UV exposure. Immediately after irradiation ($t=0$), the film is opaque and the transmission is near zero. As time evolves, the system undergoes significant changes and after waiting long enough ($t \to \infty$), the system stabilizes and the film becomes more transparent. This is illustrated in Fig. 7 where one sees that the level of light transmission given by the ratio I_T/I_0 increases by a factor of almost 5. A more detailed description of the kinetic processes leading to such an increase in the light transmission

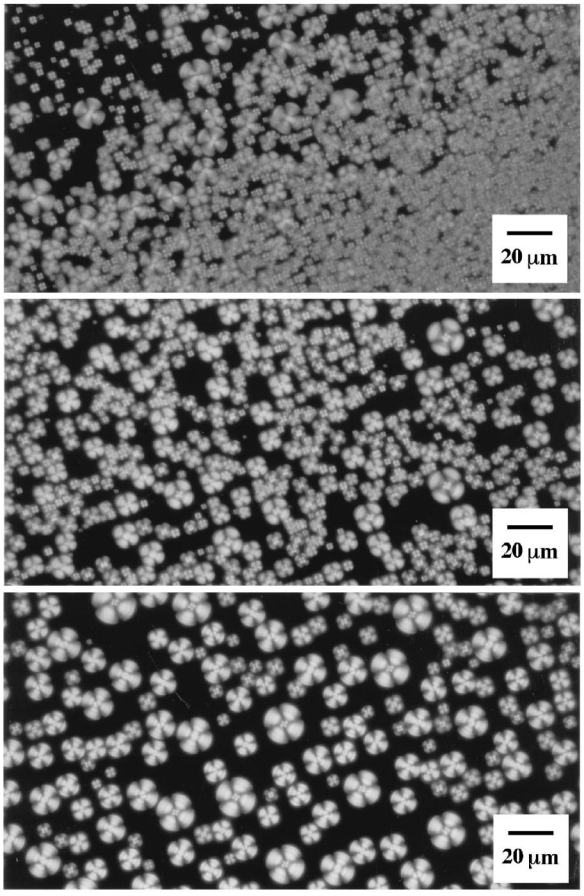

FIG. 8. Optical micrographs ($P \perp A$) of PEHA/E7 (50:50) films as a function of time elapsed after UV exposure. Top: $t=1$ min; middle: $t=30$ min; bottom: $t=15$ h.

with time will be the subject of a future communication. We give only a brief illustration of this behavior via the three optical micrographs in Fig. 8 taken at $t=1$ min, $t=30$ min, and $t=15$ h after UV irradiation.

The size and the number of droplets per unit volume clearly change from a high scattering state to a low scattering state. Starting from a great number of small droplets (~ 1 μm), the morphology of the film quickly evolves to a small number of large droplets (~ 20 μm). A two-step process seems to take place. First coalescence of neighboring drops of small size occurs, followed by a diffusion of medium size particules. The low viscosity of PEHA at room temperature ($T_{g_{PEHA}} \sim -62\,^{\circ}\mathrm{C}$) allows migration of the LC molecules into the polymer rich phase, so that coalescence of medium size droplets happens. After 12 h, the morphology of the film does not change anymore. These morphology changes can be interpreted in terms of relaxation processes of the polymer chains leading to drastic modifications in the film structure. Therefore the size, density, and spatial distribution of the LC droplets evolve in a direction that is less favorable for electro-optical applications.

IV. CONCLUSIONS

The phase behavior of 2-EHA/E7 blends in the polymerized and unpolymerized states was studied by DSC and polarized optical microscopy. The experimental phase diagrams exhibit typical UCST shapes. The (N+I) miscibility gap, as well as a single isotropic phase, was observed for both systems. For the polymerized system, the existence of an (I+I) miscibility gap has been clearly shown. The phase diagrams obtained were analyzed in terms of a classical model based on a combination of the Flory-Huggins and Maier-Saupe theories. Good agreement between experimental observations and theoretical predictions was obtained. From the DSC data, the LC solubility limit in the polymer matrix, γ, and the fractional amount of LC contained in the nematic droplets, δ, were determined. The morphology and the scattering properties of PDLC films including 50 wt % LC were studied by light transmission and POM as a function of time elapsed after UV exposure. Relaxation processes related to coalescence and diffusion of the nematic droplets have been observed, resulting in a drastic change of the size, spatial distribution, and number density of the LC droplets.

ACKNOWLEDGMENTS

The authors are indebted to Professor M. Benmouna for enlightening discussions. The authors gratefully acknowledge the financial support of the MENRT, the Région Nord-Pas de Calais, the FEDER, and the CNRS.

[1] P.S. Drzaic, *Liquid Crystal Dispersions* (World Scientific, Singapore, 1995).
[2] G.P. Crawford and S. Zumer, *Liquid Crystals in Complex Geometries* (Taylor and Francis, London, 1996).
[3] C. Serbutoviez, J.G. Kloosterboer, H.M.J. Boots, and F.J. Touwslager, Macromolecules **29**, 7690 (1996).
[4] F. Roussel, J.-M. Buisine, U. Maschke, and X. Coqueret, Liq. Cryst. **24**, 555 (1998).
[5] C. Shen and T. Kyu, J. Chem. Phys. **102**, 556 (1995).
[6] W.-K. Kim and T. Kyu, Mol. Cryst. Liq. Cryst. Sci. Technol., Sect. A **250**, 131 (1994).
[7] T. Kyu, C. Shen, and H.-W. Chiu, Mol. Cryst. Liq. Cryst. Sci. Technol., Sect. A **287**, 27 (1996).
[8] T. Kyu, I. Illies, C. Shen, and Z. L. Zhou, in *Liquid-Crystalline Polymer Systems—Technological Advances*, edited by A.I. Isayev, T. Kyu, and S.Z.D. Cheng, ACS Symposium Series No. 632 (American Chemical Society, Washington, DC, 1996), Chap. 13.
[9] F. Benmouna *et al.*, Macromol. Theory Simul. **7**, 599 (1998).
[10] L. Carpaneto, A. Ristagno, P. Stagnaro, and B. Valenti, Mol. Cryst. Liq. Cryst. Sci. Technol., Sect. A **290**, 213 (1996).
[11] W. Ahn, C.Y. Kim, H. Kim, and S.C. Kim, Macromolecules **25**, 5002 (1992).
[12] F. Benmouna *et al.*, J. Polym. Sci. Part B: Polym. Phys. **37**, 1841 (1999); Macromolecules **33**, 960 (2000).
[13] G.W. Smith, Phys. Rev. Lett. **70**, 198 (1993).
[14] Y. Hirai, S. Niiyama, H. Kumai, and T. Gunjima, Proc. SPIE **1257**, 2 (1990).
[15] C. Grand, M.F. Achard, and F. Hardouin, Liq. Cryst. **22**, 287 (1997).
[16] K. Amundson, A. van Blaaderen, and P. Wiltzius, Phys. Rev. E **55**, 1646 (1997).
[17] P.J. Flory, *Principles of Polymer Chemistry* (Cornell University Press, Ithaca, NY, 1965).
[18] W. Maier and A. Saupe, Z. Naturforsch. A **14**, 882 (1959); **15**, 287 (1960).
[19] F. Roussel, J.-M. Buisine, U. Maschke, and X. Coqueret, Mol. Cryst. Liq. Cryst. Sci. Technol., Sect. A **299**, 321 (1997).
[20] Value given by Merck Ltd, Merck House, Poole, Great Britain.
[21] F. Roussel, Ph.D. thesis, Université du Littoral-Côte d'Opale, France, 1996.
[22] The N-I transitions observed for the PEHA/E7 systems, are quite broad leading to great uncertainties in the determination of the temperature onset.
[23] H.S. Kitzerow, Liq. Cryst. **16**, 1 (1994).
[24] J.E. Proust, L. Ter-Minassian-Saraga, and E. Guyon, Solid State Commun. **11**, 1127 (1972).
[25] G.P. Crawford, R.J. Ondris-Crawford, J.W. Doane, and S. Zumer, Phys. Rev. E **53**, 3647 (1996).
[26] K.R. Amundson and M. Srinivasarao, Phys. Rev. E **58**, R1211 (1998); K.R. Amundson, *ibid.* **58**, 3273 (1998).
[27] A. Dubault, C. Casagrande, and M. Veyssie, Mol. Cryst. Liq. Cryst. Lett. **72**, 189 (1982).
[28] G. ten Brinke and F.E. Karasz, Macromolecules **17**, 815 (1984).
[29] R.S. Barnum, S.H. Goh, J.W. Barlow, and D.R. Paul, J. Polym. Sci., Polym. Lett. Ed. **23**, 395 (1985).
[30] G.W. Smith and N.A. Vaz, Liq. Cryst. **3**, 543 (1988); G.W. Smith, Mol. Cryst. Liq. Cryst. **180B**, 201 (1990).
[31] U. Maschke, F. Roussel, J.-M. Buisine, and X. Coqueret, J. Therm. Anal. Cal. **51**, 737 (1998).
[32] U. Maschke, X. Coqueret, and C. Loucheux, J. Appl. Polym. Sci. **56**, 1547 (1995).